2010

Direct scattered growth of MWNT on Si for high performance anode material in Li-ion batteries

Pengfei Gao
Shanghai Jiao Tong University

Yanna Nuli
University of Wollongong, yanna@uow.edu.au

Yu-Shi He
Shanghai Jiao Tong University

Andrew I. Minett
The University Of Sydney, aminett@uow.edu.au

Jiazhao Wang
University of Wollongong, jiazhao@uow.edu.au

See next page for additional authors

http://ro.uow.edu.au/engpapers/3570

Authors

Pengfei Gao, Yanna Nuli, Yu-Shi He, Andrew I. Minett, Jiazhao Wang, Jun Yang, and Jun Chen

Direct scattered growth of MWNT on Si for high performance anode material in Li-ion batteries†

Pengfei Gao,[a] Yanna Nuli,[a] Yu-Shi He,[a] Jiazhao Wang,[c] Andrew I. Minett,[b] Jun Yang*[a] and Jun Chen*[b]

A novel Si-MWNT nanocomposite synthesized *via* a CVD process shows a high reversible capacity of over 1500 mAh g^{-1} and stable cycling performance, which can be ascribed to the maintenance of a good conductive network by means of the direct scattered growth and pinning of MWNTs on Si particles.

The increase of energy density is a key point for extending the application range of lithium-ion batteries, especially for electric/hybrid vehicles. Silicon is one of the most attractive anode materials for lithium batteries on account of its low discharge potential and the well-known highest theoretical capacity of about 4200 mAh g^{-1} corresponding to the fully lithiated composition of Li$_{4.4}$Si,[1] which is more than ten times higher than that of commercial graphite anodes (372 mAh g^{-1}).[2] However, silicon-based electrodes suffer from very poor cyclability due to loss of electronic contact between the active particles resulting from silicon's volume changes by 400% upon insertion and extraction of lithium.[3] Research results have confirmed that the decrease of particle size of the Li-storage hosts can significantly improve the electrochemical cycling behavior due to the reduced absolute volume change and weaker pulverization tendency.[4–6]

In order to improve the electrode stability, nano-size silicon is homogeneously dispersed within a suitable matrix resulting in a nanocomposite, in which the second phase component acts as a buffering matrix to accommodate the large volume changes upon cycling. Among the different matrix materials considered, carbon is a good candidate due to its relatively low mass, good electronic and ionic conductivity, reasonable Li-insertion capability, small volume expansion, softness and compliance.[7] Various methods have been employed for preparing Si/C composite anodes.[8,9] Dahn *et al.* appear to have been the first to prepare Si/C composites from thermal pyrolysis of various polymers containing silicon and carbon, such as polymethylphenylsiloxane (PMPS) or polyphenyl-sesquisiloxane (PPSSO) in the temperature range of 900–1300 °C.[10] Lately, the Si@C composites with core/shell structure have aroused great interest because the complete carbon shell could buffer the volumetric changes of Si particles and maintain the electric contact.[11,12] Ng *et al.* reported on the synthesis of carbon-coated Si nanocomposite prepared using a spray pyrolysis method, exhibiting a capacity of 1489 mAh g^{-1} after 20 cycles.[13] Hu *et al.* prepared core/shell Si@C nano-composites by hydrothermal treatment of a dispersion of Si nanoparticles and glucose in water, followed by heat treatment in nitrogen.[14,15] This material presented good cycling performance with the help of vinylene carbonate (VC) electrolyte additive, but it was not stable in the conventional electrolyte without VC. Up to now, the cycling performance of core/shell Si@C composites is still unsatisfactory for industrial applications, perhaps due to the destruction of the carbon shell upon silicon volume variations during cycling.[16] More durable composite architectures with strong adherence between silicon and carbon need to be developed to guarantee the close electric contact.

More recently, great efforts have been made toward the syntheses of nanocomposites of inorganic materials and carbon nanotubes (CNTs),[17–19] with the aim of exploiting the unique properties of CNTs, such as the high aspect ratio, low mass, flexibility, high mechanical strength, and high electrical and thermal conductivities for applications in lithium ion batteries.[20,21] Shu *et al.* demonstrated a cage-like CNTs/Si composite with a reversible capacity of 940 mAh g^{-1} and improved cycling performance for 20 cycles, where micro-size Si particles were enwrapped by the coiled CNTs *via* a catalytic chemical vapor deposition (CVD) process.[22] Related work was published by Kim *et al.*, wherein the improved cyclability has been attributed to the conductive buffering role of the CNTs layer and the void space within it, which alleviated breakdown of the conductive network in Si negative electrodes.[23] However, the inhomogeneous Ni catalyst deposits prepared in the electroless plating process gave rise to two different types of CNTs and even caused unsuccessful growth of those in some samples. Meanwhile, the number of charge–discharge cycles was limited to only 12. Another kind of one dimensional carbon material, carbon nanofibers (CNFs), were also investigated as candidates for Si/C composites through a CVD approach,[24,25] but showed less stable cycling performance, perhaps owing to their intrinsical

[a] *Institute of Electrochemical and Energy Technology, Department of Chemical Engineering, Shanghai Jiao Tong University, Shanghai, 200240, China. E-mail: yangj723@sjtu.edu.cn; Fax: +86-21-5474 7667; Tel: +86-21-5474 7667*
[b] *Intelligent Polymer Research Institute, ARC Centre of Excellence for Electromaterials Science, AIIM Facility, Innovation Campus, University of Wollongong, Wollongong, NSW 2522, Australia. E-mail: junc@uow.edu.au; Fax: +61-2-4221 3114; Tel: +61-2-4221 3781*
[c] *ARC Centre of Excellence for Electromaterials Science, Institute of Semiconducting and Electronic Materials, AIIM Facility, Innovation Campus, University of Wollongong, Wollongong, NSW 2522, Australia*

† Electronic supplementary information (ESI) available: Experimental details, SEM images of the Si/MWNT mixture, Raman spectra and thermogravimetry profiles of the Si-MWNT composite and pure Si powder, reversible capacities of the Si-MWNT composite and Si/MWNT mixture and schematic illustration of structural changes for different Si-CNT materials. See DOI: 10.1039/c0cc02870c
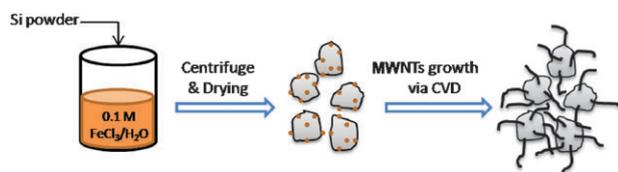
Scheme 1 Schematic procedures for the preparation of Si-MWNT composite.

deficiencies, *e.g.* lower mechanical strength and toughness compared to those of CNTs.[26]

Herein, we propose the use of a novel nanoarchitectured Si-MWNT composite as a high performance anode material, in which mutiwalled carbon nanotubes (MWNTs) were directly grown on the surface of Si nanoparticles *via* a simplified CVD method discarding the electroless plating procedure that is complicated and difficult to control. The obtained MWNTs are much more uniform and serve as a kind of "electronic wire" which effectively connect Si nanoparticles. This Si-MWNT composite shows superior cycling properties, delivering a reversible capacity of 1501 mAh g^{-1} after 20 cycles and good rate performance.

As shown in Scheme 1, in a typical experiment, Si powder with the modification of iron ion was prepared by surface adsorption technique and separated in a centrifuge at a speed of 6000 rpm. After being dried in a vacuum oven at 100 °C for half an hour, the iron modified Si powder was put into the furnace and was ready for the chemical vapor deposition of MWNTs. During the CVD process, the iron(III) was first reduced to iron nanoparticles under hydrogen gas flow (30 mL per min) at 550 °C. Then MWNTs were deposited onto Si particles at 750 °C under $H_2/C_2H_2/Ar$ (5/30/200 cc/min) mix-gas flow for 20 min. The Fe catalyst remained after the CVD process and was confirmed by EDX analysis. For comparison, the Si/MWNT mixture was also prepared by ball milling method with the same silicon content.

Scanning and transmission electron microscopy images of the Si-MWNT composite (Fig. 1) show a successful scattered growth of MWNTs from Si particles to establish a MWNT network among Si particles in the sizes ranging from several

tens to hundreds of nanometres. The MWNTs deposited on Si have diameters of 10–30 nm (Fig. 1b and c), well matched with the Si particle size and comparable to the commercial MWNTs used in the Si/MWNT mixture (Fig. S1 in ESI†). A clear difference can be detected between the two samples from Fig. 1 and Fig. S1 in ESI†. The HR-TEM micrograph of the Si-MWNT composite (Fig. 1d) demonstrates the catalytic growth of MWNTs from the surface of Si with strong adherence, and they have not been detached from Si particles by high power ultrasonication. This would play a key role for stability in the battery performance. For the Si/MWNT mixture, however, the Si is just entwined with MWNTs and the contact is relatively loose, as exhibited in Fig. S1b. Furthermore, the Raman spectroscopy of the Si-MWNT composite is exhibited in Fig. S2 in ESI†, where wide D and G bands around 1310 and 1590 cm^{-1} correspond to the characteristic peaks of MWNTs.[27] The content of MWNTs in the Si-MWNT composite was determined to be 31% (mass weight) *via* TGA analysis (Fig. S3 in ESI†).

Electrochemical tests revealed a large reversible capacity of this Si-MWNT composite as high as 1592 mAh g^{-1} with an initial coulombic efficiency of 76.9% (Fig. 2a). The capacity rose slightly for the first several cycles, which my be related to the gradual activation of Si host, and then stayed above 1500 mAh g^{-1} for 20 cycles. By contrast, the Si/MWNT mixture exhibited a initial capacity of only 1041 mAh g^{-1} and showed rapid capacity decay (Fig. S4 in ESI†). This would be attributed to the poor electronic conductivity and resulting low utilization of active material. We also evaluated the rate performance of the Si-MWNT composite at different current densities after 40 cycles of galvanostatic charge–discharge. As shown in Fig. 2b, the composite retains about 700 mAh g^{-1} even after 80 cycles at a high current density of 500 mA g^{-1} and recovers to 909 mAh g^{-1} when the current density turns back. On the other hand, neither the Si/MWNT mixture nor pure Si powder can stand such high current densities.

After cycling, A.C. impedance spectroscopy of the cells was taken to study the interface property. All three electrodes exhibited Nyquist plots consisting of a depressed semicircle at high frequency range, as presented in Fig. 3, which is correlated with the electron transfer resistance on the electrode
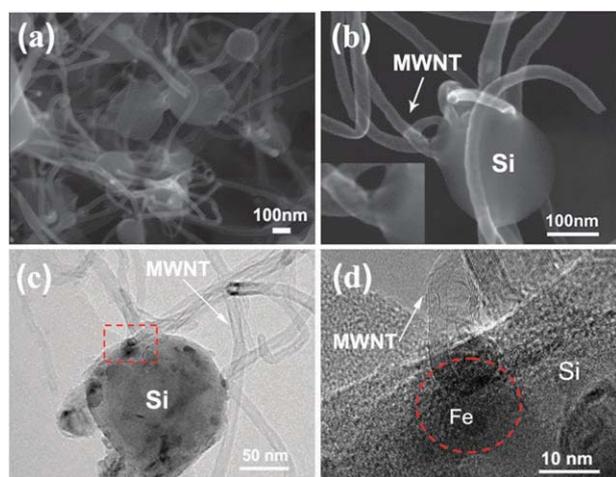

Fig. 1 SEM (a, b) and TEM (c, d) micrographs of the Si-MWNT composite (b inset, c and d show the Si-MWNT junctions).
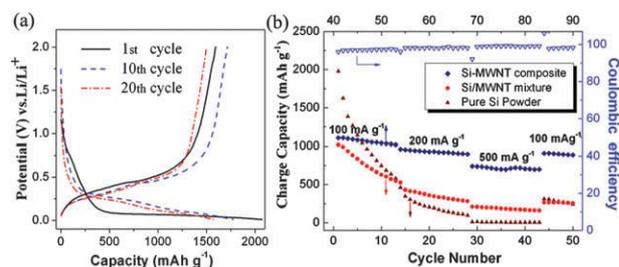

Fig. 2 (a) Galvanostatic charge–discharge profiles of the Si-MWNT composite at the 1st, 10th, and 20th cycle. (b) Rate performances of Si-MWNT composite, Si/MWNT mixture and pure Si powder at different current densities from 100 mA g^{-1} to 500 mA g^{-1} and then back to 100 mA g^{-1}. Note that the Si-MWNT composite was tested from the 41st to the 90th cycle (including the coulombic efficiency), while the Si/MWNT mixture and pure Si powder from the 1st to the 50th cycle, as indicated in the figure with different scales.
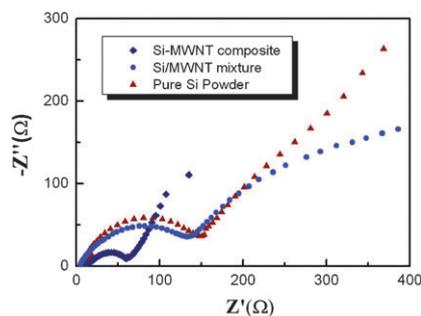
Fig. 3 Nyquist plots of the cells with Si-MWNT composite, Si/MWNT mixture and pure Si powder electrodes after cycling.

interface.[28] The Si-MWNT composite provides the smallest diameter of high frequency semicircle, indicating the good electronic contact maintained after repeated lithium insertion and extraction process, which benefits from the strong adherence and thus direct electronic connection of MWNTs on the surface of Si as shown in Fig. 4. By contrast, the Si/MWNT mixture and pure silicon display larger electron transfer resistance due to the poor electronic contact during cycling. Scheme S1 in ESI† further illustrates the sample structures and their possible evolutions after cycling for the three kinds of Si-CNT materials. A cage-like CNT-Si composite formed by micro-sized Si particles and densely grown CNT (Scheme S1 A), such as reported in ref. 22, may form a thick solid electrolyte interphase (SEI) film merging the CNTs, decreasing the electronic conductivity of Si particles. In addition, coarse Si particles will break into smaller fragments due to the strong mechanical stress caused by the drastic volume change and result in a loss of local electronic connection.[3] On the other hand, a stable conductive network between the active nanoparticles can still be maintained for the present Si-MWNT composite (Scheme S1 B), leading to excellent cycling and rate performances. However, physical mixing of MWNTs cannot prevent the breakdown of the conductive network in silicon electrodes (Scheme S1 C).

In summary, a Si-MWNT nanocomposite was successfully synthesized by direct scattered growth of MWNTs on the surface of Si nanoparticles *via* a CVD process using C_2H_2 as carbon source and Fe catalyst. This composite presents a high reversible capacity of 1592 mAh g^{-1} and good cycling stability even at large current densities of 500 mA g^{-1}, which can be ascribed to the maintenance of a good electronic conducting network due to the robust adherence of MWNTs on Si and the

excellent flexibility of MWNTs, which can accommodate the severe volume change of Si upon lithium insertion and extraction. This superior performance makes the Si-MWNT composite a promising anode material for lithium ion batteries.

Notes and references

1 B. A. Boukamp, G. C. Lesh and R. A. Huggins, *J. Electrochem. Soc.*, 1981, **128**, 725–729.
2 S. Megahed and B. Scrosati, *J. Power Sources*, 1994, **51**, 79–104.
3 C. K. Chan, H. Peng, G. Liu, K. McIlwrath, X. F. Zhang, R. A. Huggins and Y. Cui, *Nat. Nanotechnol.*, 2008, **3**, 31–35.
4 H. Li, X. Huang, L. Chen, Z. Wu and Y. Liang, *Electrochem. Solid-State Lett.*, 1999, **2**, 547–549.
5 M. Winter and J. O. Besenhard, *Electrochim. Acta*, 1999, **45**, 31–50.
6 J. L. Wang and J. Yang, in *Encyclopedia of Electrochemical Power Sources*, ed. C. D. Juergen Garche, Patrick Moseley, Zempachi Ogumi, David Rand and Bruno Scrosati, Elsevier, Amsterdam, 2009, vol. 5, pp. 225–236.
7 W. R. Liu, J. H. Wang, H. C. Wu, D. T. Shieh, M. H. Yang and N. L. Wu, *J. Electrochem. Soc.*, 2005, **152**, A1719–A1725.
8 J. Yang, B. F. Wang, K. Wang, Y. Liu, J. Y. Xie and Z. S. Wen, *Electrochem. Solid-State Lett.*, 2003, **6**, A154–A156.
9 A. Magasinski, P. Dixon, B. Hertzberg, A. Kvit, J. Ayala and G. Yushin, *Nat. Mater.*, 2010, **9**, 353–358.
10 A. M. Wilson, J. N. Reimers, E. W. Fuller and J. R. Dahn, *Solid State Ionics*, 1994, **74**, 249–254.
11 P. F. Gao, J. W. Fu, J. Yang, R. G. Lv, J. L. Wang, Y. N. Nuli and X. Z. Tang, *Phys. Chem. Chem. Phys.*, 2009, **11**, 11101–11105.
12 Y. Xu, G. Yin, Y. Ma, P. Zuo and X. Cheng, *J. Mater. Chem.*, 2010, **20**, 3216–3220.
13 S. H. Ng, J. Wang, D. Wexler, K. Konstantinov, Z. P. Guo and H. K. Liu, *Angew. Chem., Int. Ed.*, 2006, **45**, 6896–6899.
14 R. Demir Cakan, M. M. Titirici, M. Antonietti, G. Cui, J. Maier and Y. S. Hu, *Chem. Commun.*, 2008, 3759–3761.
15 Y. S. Hu, R. Demir-Cakan, M. M. Titirici, J. O. Müller, R. Schlögl, M. Antonietti and J. Maier, *Angew. Chem., Int. Ed.*, 2008, **47**, 1645–1649.
16 L. W. Su, Z. Zhou and M. M. Ren, *Chem. Commun.*, 2010, **46**, 2590–2592.
17 M. S. Park, S. A. Needham, G. X. Wang, Y. M. Kang, J. S. Park, S. X. Dou and H. K. Liu, *Chem. Mater.*, 2007, **19**, 2406–2410.
18 W. Wang and P. N. Kumta, *J. Power Sources*, 2007, **172**, 650–658.
19 H. X. Zhang, C. Feng, Y. C. Zhai, K. L. Jiang, Q. Q. Li and S. S. Fan, *Adv. Mater.*, 2009, **21**, 2299–2304.
20 J. Chen, A. I. Minett, Y. Liu, C. Lynam, P. Sherrell, C. Wang and G. G. Wallace, *Adv. Mater.*, 2008, **20**, 566–570.
21 J. Chen, J. Z. Wang, A. I. Minett, Y. Liu, C. Lynam, H. Liu and G. G. Wallace, *Energy Environ. Sci.*, 2009, **2**, 393–396.
22 J. Shu, H. Li, R. Z. Yang, Y. Shi and X. J. Huang, *Electrochem. Commun.*, 2006, **8**, 51–54.
23 T. Kim, Y. H. Mo, K. S. Nahm and S. M. Oh, *J. Power Sources*, 2006, **162**, 1275–1281.
24 H. P. Liu, W. M. Qiao, L. Zhan and L. C. Ling, *New Carbon Mater.*, 2009, **24**, 124–130.
25 S. M. Jang, J. Miyawaki, M. Tsuji, I. Mochida and S. H. Yoon, *Carbon*, 2009, **47**, 3383–3391.
26 J. M. Park, D. S. Kim, S. J. Kim, P. G. Kim, D. J. Yoon and K. L. DeVries, *Composites, Part B*, 2007, **38**, 847–861.
27 P. Delhaes, M. Couzi, M. Trinquecoste, J. Dentzer, H. Hamidou and C. Vix-Guterl, *Carbon*, 2006, **44**, 3005–3013.
28 R. Ruffo, S. S. Hong, C. K. Chan, R. A. Huggins and Y. Cui, *J. Phys. Chem. C*, 2009, **113**, 11390–11398.
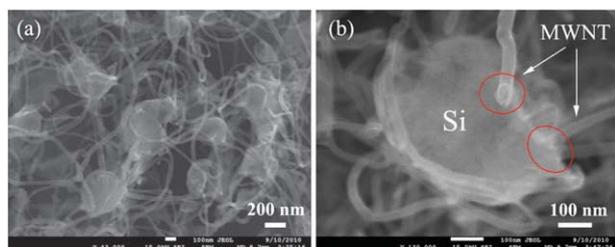
Fig. 4 SEM micrographs of a Si-MWNT composite electrode after 50 cycles. The relatively blurry particle morphology (b) may be related to the SEI film. The circled areas highlight the Si-MWNT junctions.